T3-D3-4 : Norm-oriented mesh-adaption analysis for a third-order accurate Euler model

A. Carabias[b], A. Loseille[a], A. Dervieux[b]

[a]*INRIA, Projet Gamma, Domaine de Voluceau, Rocquencourt, BP 105, 78153 Le Chesnay Cedex, France.*
[b]*INRIA, Projet Tropics, 2004 route des lucioles - BP 93, 06902 Sophia Antipolis Cedex, France*

Abstract

In this report a central-ENO approximation for the unsteady 2D Euler equations is considered. The scheme is third-order accurate on irregular unstructured meshes. First, the paper concentrates on a method for a goal-oriented mesh adaption. For this purpose, an *a priori* implicit error analysis for this CENO scheme is proposed. It allows to get an estimate depending on the reconstruction error. In contrast to linear reconstruction error, specifying a stretching direction minimising a third order reconstruction error is not an immediate task. Then an optimum problem for the mesh metric is obtained and analytically solved. Second, a new analysis, the norm-oriented analysis is applied to the same context and new optimality conditions are produced.

Key words: Computational Fluid Dynamics, high order approximation, mesh adaptation

1. Introduction

High order approximations in Computational Mechanics are an attracting mean for obtaining computations with smaller approximation errors, or, more importantly nowadays, for obtaining computations with less computer time, thanks to the use of coarser meshes.

However high order approximations do not reduce mesh fineness constraints related to the size and number of details in the different solution fields (from monotony changes to stiff variations). Disobeying these constraints leads to low order errors and possibly to oscillations.

A well known cure to that latter limitation is the application of mesh adaptive strategies. In the case of isotropic mesh adaption, the h, p methods which control together mesh local size and scheme local accuracy have shown an impressive efficiency in adressing mechanical problems involving many details and scales.

When the fields under study involve structures of lower dimension, like discontinuity curves in

2D, an anisotropic mesh adaption may be necessary.

Hessian-based error estimates combined with a metric for representing the mesh showed efficiency for second order finite-element-type approximations (see [7] for a recent example). This association is rather naturally derived since the optimal metric is a scalar factor times the Hessian of the variable chosen as sensor, that is the main bilinear term of its P_1-interpolation error.

Then the extension to third order accuracy appears as the next step. Looking for P_2-interpolation error of sensor leads to consider the trilinear third-order term of its Taylor series. It is possible to imagine mesh adaptation controlled directly by these third order derivatives. See for example [**?**]. In the present paper we shall less ambitiously propose to convert the trilinear information in to a bilinear one, a pseudo-Hessian-based error model.

Mesh adaptation based on interpolation error take into account very incompletely approximation error. A more accurate problematic is to address the reduction of the error committed on a scalar output. Initially restricted to interpolation errors, anisotropic error estimates are now available for goal-oriented formulations, see [12],[2],[15]. In particular, *a priori estimates* have become an efficient tool for addressing mesh adaptation issues for steady Euler flows [20], then for unsteady Euler flows [6], and more recently for steady and unsteady Navier-Stokes ones [5]. In these papers, the error analysis follows the so-called *a priori* implicit error method, dealing with a discrete invertible system for the deviation between discrete solution and a projection of the continuous one. Such *a priori* estimates were obtained for a second-order mixed-element-volume approximation close to the usual $\mathcal{P}^1$ finite element. Promises given by theory were kept by numerical demonstrators, showing second-order convergence for shocked flows. The theory also predicts higher-order convergence for the higher-order interpolation of singular flows. A necessary condition is the application of an anisotropic strategy, involving an anisotropic error estimate.

Goal-oriented analysis allows to reduce the error on a scalar output. But in many applications, the user needs to control the overall approximation error, for example reducing the L^2 error of approximation. This ca be addressed by an extension of the goal-oriented approach, the norm-oriented one [8, 19]. The main idea is to build a so-called corrector for representing this approximation error.

In this paper we consider a central-ENO approximation for the Euler equations. The scheme is third-order accurate on irregular unstructured meshes.

We first present a mesh adaption method based on an interpolation error. In [9], Weiming Cao

proposes a first approximation of this error with stretching directions. In the present paper, we propose to replace the application of third derivative to a mesh size by the power 3/2 of a pseudo-Hessian times mesh size. Then an optimal mesh-metric is derived analytically. For solving the resulting mesh optimality system, we discretise it and apply a fixed point for steady flows. The new method is applied to a scramjet flow.

Then we address a goal-oriented problematic. An approximation error analysis need be performed. The implicit error method introduced for a second-order approximation in [16] is extended to the third-order CENO. The resulting *a priori* error analysis is a kind of dual of the *a posteriori* analysis of Barth and Larson [4]. The error is expressed in terms of the application of third derivative to a mesh size. Again a pseudo-Hessian operator is introduced. Then an optimisation problem for the mesh metric is obtained and analytically solved. The extension to a norm-oriented analysis is then presented by introducing a Defect-Correction based corrector which play the role of the approximation error.

2. Numerical approximation of a function

2.1. Quadratic-interpolation error in 1D

We are forst interested by evaluating the quadratic-interpolation error on a mesh $\mathcal{M}$ of interval $[0,1]$ parameterized by a continuous mesh size $m(x)$. On each interval $]x_{i-1}, x_i[$ with $x_{i-1} = \frac{1}{N}\int_0^{i-1} m^{-1}(x)dx$ and $u - \Pi_{\mathcal{M}}u$ erreur d'interpolation P_k:

$$\int_0^1 |u - \Pi_{\mathcal{M}}u|dx \approx \int_0^1 |e_{\mathcal{M}}(x)|dx = \int_0^1 (m^{k+1}|\delta^{-k-1}D_h^{k+1}\mathbf{u}_\delta|)dx.$$

où $\mathbf{u}_\delta = (u(i\delta)))_{i\in Z)}$ et $D_h\mathbf{u}_\delta = (u((i+1)\delta) - u(i\delta))_{i\in Z)}$. δ est plus petit que la taille de maille minimale $\min m$.

Le quotient différentiel $\delta^{-k-1}D_h^{k+1}\mathbf{u}_\delta$: proche de $\frac{\partial^2 u}{\partial x^2}$ là où u est régulier, borné dans $L^{\mathbf{1/k}}$ (indép. de δ) là où u est discontinu.

Maillage optimal pour un nombre donné de nœuds

$$\min_{\mathcal{M}} \int_0^1 |e_{\mathcal{M}}(x)|ds \;\; ; \;\; \int m(x)^{-1}\, dx \;=\; N\;. \tag{1}$$
$$\Rightarrow m_{opt}(x) = C(N)|(\delta^{-k-1}D_h^{k+1}\mathbf{u}_\delta(x))|^{\frac{-1}{k+1}}.$$

$$m^{-2}_{opt,2D}(x) = C(N)^{-2}|\frac{D^2_h \mathbf{u}_\delta(x)}{\delta^2}| \quad ; \quad m^{-2}_{opt,3D}(x) = C(N)^{-2}|\frac{D^3_h \mathbf{u}_\delta(x)}{\delta^3}|^{\frac{2}{3}}$$

De plus l'erreur correspondante dans L^1 s'écrit:

$$\left(\int_0^1 |e_{\mathcal{M}_{opt}}(x)|ds\right) = \frac{1}{N^{k+1}} \left(\int |\delta^{-k-1} D^{k+1}_h \mathbf{u}_\delta|^{\mathbf{1/k+1}}\right)^{\frac{k^2+k+1}{k+1}} < \frac{K}{N^{k+1}}$$

précision à l'ordre $k+1$ en dépit de la discontinuité.

2.2. Quadratic-interpolation error

Let f be a smooth mapping from $\mathbb{R}^n$ to $\mathbb{R}^p$.

2.3. Taylor series

The Taylor theorem for f writes:

$$f(\mathbf{x}+\delta\mathbf{x}) = f(\mathbf{x}) + \sum_{k=1}^{k=m} \frac{1}{i!} D^k f(\mathbf{x})(\delta\mathbf{x})^k + R_{k+1} \quad \text{with} \quad ||R_{k+1}|| = O(||\delta\mathbf{x}||^{k+1}).$$

Here the Fréchet derivative $D^k f(\mathbf{x})$ of f at point $\mathbf{x}$ is a tensor or multi-linear application or an element of $\mathcal{L}(\mathbb{R}^k;\mathbb{R}^p)$. Due to the Leibnitz formula, $D^k f(\mathbf{x})$ is a symmetric tensor in the sense that:

$$D^k f(\mathbf{x}) \cdot (\xi_1, \xi_2, ..., \xi_k) = D^k f(\mathbf{x}) \cdot (\xi_{\sigma_1}, \xi_{\sigma_2}, ..., \xi_{\sigma_k})$$

for any permutation $\sigma :\mapsto \sigma_i$ of the set $\{1, 2, ..., k\}$. In case the vector $\xi_i = \xi$ for all $1 \leq i \leq k$, we simply write:

$$D^k f(\mathbf{x}) \cdot (\xi, \xi, ..., \xi) = D^k f(\mathbf{x}) \cdot (\xi)^k.$$

For example, for $n = 2$, $p = 1$

$$D^2 f(\mathbf{x})(\delta\mathbf{x})^2 = \frac{\partial^2 f}{\partial x_1^2}\delta\mathbf{x}_1^2 + 2\frac{\partial^2 f}{\partial x_1 \partial x_2}\delta\mathbf{x}_1\delta\mathbf{x}_2 + \frac{\partial^2 f}{\partial x_2^2}\delta\mathbf{x}_2^2$$

$$D^3 f(\mathbf{x})(\delta\mathbf{x})^3 = \frac{\partial^3 f}{\partial x_1^3}\delta\mathbf{x}_1^3 + 3\frac{\partial^3 f}{\partial x_1^2 \partial x_2}\delta\mathbf{x}_1^2\delta\mathbf{x}_2 + 3\frac{\partial^3 f}{\partial x_1 \partial x_2^2}\delta\mathbf{x}_1\delta\mathbf{x}_2^2 + \frac{\partial^3 f}{\partial x_2^3}\delta\mathbf{x}_2^3.$$

The norm of $D^k f(\mathbf{x})$ is defined as

$$||D^k f(\mathbf{x})|| = sup\{|D^k f(\mathbf{x}) \cdot (\xi_1, \xi_2, ..., \xi_k)|; ||\xi_i|| \leq 1, 1 \leq i \leq k\}$$

For $p = 1$ the estimate on R_{k+1} can be refined by using the expression of the general term:

$$R_{k+1} \preceq |\frac{1}{k!} D^{k+1} f(\mathbf{x})(\delta\mathbf{x})^{(k+1)}|$$

where $\preceq$ means that the inequality is true at the limiting case of $|\delta\mathbf{x}|$ infinitely small.

2.4. Lagrange interpolation

Given an integer $k \geq 1$, denoting P_k the space of polynomials of degree $\leq k$ defined over $\mathbb{R}^n$, we define $N = N(k) = \dim P_k$. A set $\Sigma = \{a_i\}_{i=1}^N$ of N distinct points a_i of $\mathbb{R}^n$ form a $k-$*unisolvent set* if , given any real numbers α_i, $1 \leq i \leq N$, there exists one and only one polynomial $p \in P_k$ such that

$$p(a_i) = \alpha_i, \quad 1 \leq i \leq N.$$

Three notions introduced in [11] will be useful in our modelization of anisotropy.

Given such a set $\Sigma = \{a_i\}_{i=1}^N$, we denote by $K(\Sigma)$ the closed convex hull of Σ. To $K(\Sigma)$ are associated two geometrical parameters:

$$h = h(\Sigma) = \text{ diameter of } K(\Sigma),), \tag{2}$$

$$\rho = \rho(\Sigma) = \sup\{ \text{ diameter of the spheres contained in } K(\Sigma)\} \tag{3}$$

If Σ is any unisolvent set with $k \leq 1$ its interior is nonempty and $\rho(\Sigma)$ is strictly positive. Let $\Sigma = \{a_i\}_{i=1}^N$ and $\hat{\Sigma} = \{\hat{a}_i\}_{i=1}^N$ be two sets of points in $\mathbb{R}^n$. We say they are *equivalent* if and only if there exists an invertible element $B \in \mathcal{L}(\mathbb{R}^n)$ such that:

$$a_i = B\hat{a}_i + b, \quad 1 \leq i \leq N.$$

If $\Sigma = \{a_i\}_{i=1}^N$ is unisolvent so is $\hat{\Sigma} = \{\hat{a}_i\}_{i=1}^N$.

In [11], it is shown that for two such equivalent $k-$unisolvent sets, we have:

$$||B|| \leq \frac{h}{\hat{\rho}} \ \ and \ \ ||B^{-1}|| \leq \frac{\hat{h}}{\rho} \ .$$

We shall be more interested by the case of a symmetric matrix B:

$$\mathcal{B} = \mathcal{R} \begin{pmatrix} \beta_1 & 0 \\ 0 & \beta_2 \end{pmatrix} {}^t\mathcal{R}. \tag{4}$$

It is then possible to measure the impact of transformation B as the effect of the involved stretching (β_1, β_2) on the shape coefficients (h, ρ):

$$h \leq max(\beta_1, \beta_2)\hat{h} \ \ ; \ \ \rho \leq min(\beta_1, \beta_2)\hat{\rho}.$$

Given a function u defined on a $k-$unisolvent set Σ, the polynomial $\tilde{u}$ is the *interpolating polynomial* of u if it is the unique polynomial of degree $\leq k$ satisfying:

$$\tilde{u}(a_i) = u(a_i), \quad 1 \leq i \leq N.$$

An error estimate for Lagrange interpolation has been established in [11]:

Theorem 1: *Let k be a fixed integer ≥ 1, and let $\Sigma = \{a_i\}_{i=1}^N$ a $k-$unisolvent set of points in $\mathbb{R}^n$. Let $K \subset \mathbb{R}^n$ be a $\Sigma-$admissible set, $u \in \mathcal{C}^{k+1}(K)$. Then, for any point $x \in K$ and any integer m with $0 \leq m \leq k$, one has:*

$$D^m\tilde{u}(\mathbf{x}) = D^m u(\mathbf{x}) + \frac{1}{(k+1)!}\sum_{i=1}^{N}\{D^{k+1}u(\eta_i(\mathbf{x})\cdot(a_i-\mathbf{x})^{k+1}\}D^m p_i(\mathbf{x})$$

where the p_i's are the unique polynomials of degree $\leq k$ such that

$$p_i(a_j) = \delta_{ij}, \quad 1 \leq i,j \leq N,$$

and $\eta_i(\mathbf{x}) = \theta_i\mathbf{x} + (1-\theta_i)a_i$.

Theorem 2: *Let $\Sigma = \{a_i\}_{i=1}^N$ be a $k-$unisolvent set of points of $\mathbb{R}^n$, and h and ρ defined as in (2)(3). Let $u \in \mathcal{C}^{k+1}(K)$ be given with*

$$M_{k+1} = sup||D^{k+1}u(x)||; x \in K < \infty.$$

If u is the unique interpolating polynomial of degree $\leq k$of u, we have for any integre m with $0 \leq m \leq k$,

$$sup||D^m u(x) - D^m\bar{u}(x)||; x \in K \;\leq\; CM_{k+1}\frac{h^{k+1}}{\rho^m} \;\leq\; C'M_{k+1}\frac{max(\beta_1,\beta_2)^k}{min(\beta_1,\beta_2)^m},$$

for some constants

$$C = C(n,k,m,\hat{\Sigma}) \quad , \quad C' = C'(n,k,m,\hat{\Sigma})$$

which are the same for all equivalent $k-$unisolvent sets and which can be computed one for all for a fixed $\hat{\Sigma}$.

2.5. k-Exact reconstruction

The assumption now is that the polynomial is obtained by any $k-$exact reconstruction. This case has been also addressed in [11]. The symbol $W^{k+1,p}(\Omega)$ holds for the Sobolez space equipped with the usual norm $||.||_{m,p,\Omega}$.

$$||u||_{m,p,\Omega} = \left(\sum_{l=0}^{m}||D^l u||_{p,\Omega}^p\right)^{\frac{1}{p}} \quad ; \quad |u|_{m,p,\Omega} = ||D^m u||_{p,\Omega} \quad ; \quad ||D^m u||_{p,\Omega} = \left(||D^l u(x)||^p\right)^{1/p}.$$

The Lagrange interpolation is one way, among many others, for approximating a function by a polynomial. Two important properties of it is the linearity and the $k-$exactness. These are precisely the main assumptions of a second theorem from [11]:

Theorem 3: *Let Ω be a bounded open subset of $\mathbb{R}^n$ with a continuous boundary. Let p, $1 \leq p \leq \infty$, $k \geq 0$ an integer, m a second integer such that $0 \leq m \leq k+1$. Let Π a mapping of $\mathcal{L}(W^{k+1,p}(\Omega); W^{m,p}(\Omega))$ satisfying the $k-$exactness property:*

$$\Pi u = u \quad \forall \quad u \in P_k.$$

Then for any $u \in W^{k+1,p}(\Omega)$ and for h small enough, we have:

$$||u - \Pi u||_{m,p,\Omega} \ \leq \ C|u|_{k+1,p,\Omega} \ \frac{h^{k+1}}{\rho^m} \ \leq \ C'|u|_{k+1,p,\Omega} \ \frac{max(\beta_1,\beta_2)^k}{min(\beta_1,\beta_2)^m},$$

for some constants

$$C = C(n,k,p,\hat{\Omega},\hat{\Pi}) \quad ; \quad C' = C'(n,k,p,\hat{\Omega},\hat{\Pi})$$

which are the same for all equivalent domains Ω and which can be computed once for all in a domain $\hat{\Omega}$ equivalent to Ω.

2.6. Quadratic reconstruction error on a continuous mesh

For a quadratic reconstruction, we shall use as model for the reconstruction error the following term:

$$E_R(u) = \sup_{\delta \mathbf{x}} \sup_{\mathbf{x}} |D^3 u(\mathbf{x})(\delta \mathbf{x})^3|$$

3. Numerical approximation for PDE

3.1. Model

The 2D Euler equations in a geometrical domain Ω of boundary Γ can be written:

$$\text{Find } u \in \mathcal{V} \text{ such that } \int_\Omega v \nabla \cdot \mathcal{F}(u) \ d\ \Omega = \int_\Gamma v \mathcal{F}_\Gamma(u) \ d\ \Gamma \ \forall \ v \in \mathcal{V}. \tag{5}$$

Here $u = (u_1, u_2, u_3, u_4)$ holds for the conserved unknowns (density, moments components, energy) and $\mathcal{F}$ for the usual Euler fluxes. As right-hand side we have an integral of the various boundary fluxes $\mathcal{F}_\Gamma$ for various boundary conditions, which we do not need to detail here. Defining

$$B(u,v) = \int_\Omega v \nabla \cdot \mathcal{F}(u) \ d\ \Omega \ - \ \int_\Gamma v \mathcal{F}_\Gamma(u) \ d\ \Gamma,$$

this writes:

$$\text{Find } u \in \mathcal{V} \text{ such that } B(u,v) \ = \ 0 \ \forall \ v \in \mathcal{V}. \tag{6}$$

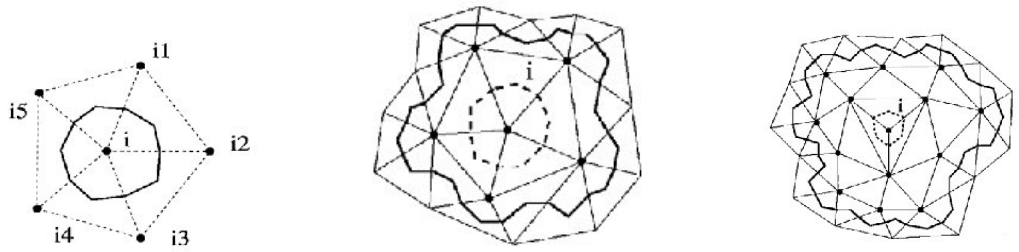

Figure 1: Dual cell and two reconstruction molecules

3.2. CENO formulation

We choose a reconstruction-based finite-volume method, getting inspired by the unlimited version of the reconstruction technique of Barth [3] and of Central-ENO (CENO) methods developed by Groth and co-workers, [14]. Concerning the location of nodes with respect to mesh elements, we prefer to minimize the number of unknowns with respect to a given mesh and therefore we keep the vertex-centered location already successfully used for second-order anisotropic (Hessian-based or Goal-oriented) mesh adaptation. The considered numerical approximation is described in details in [13]. Its main features are: (a) vertex centered, (b) dual median cells around the vertex, (c) a single mean square conservative quadratic reconstruction for each dual cell (d) Roe Riemann solver for fluxes integration, (e) explicit multi-stage time-stepping.

The computational domain is divided in triangles and in a dual tesselation in cells, each cell C_i being built around a vertex i, with limits following sections of triangle medians.

We define the discrete space $\mathcal{V}_0$ of functions that are constant on any dual cell C_i.

Let us define a reconstruction operator R_2^0 which reconstructs a function of $\mathcal{V}_0$ in each cell C_i under the form of a second-order polynomial:

$$R_2^0 u_0|_{C_i} = \mathcal{P}_i(X).$$

Given the means $(\overline{u_{0,i}}, i = 1, ...)$ of u_0 on cells i of centroid G_i, find the $c_{i,\alpha}$, $|\alpha| \leq k$ such that

$$\overline{\mathcal{P}_{i,i}} = \overline{u_{0,i}} \qquad \sum_{j \in N(i)} (\overline{\mathcal{P}_{i,j}} - \overline{u_{0,j}})^2 = Min$$

with

$$\mathcal{P}_i(x) = \overline{u_{0,i}} + \sum_{|\alpha| \leq k} c_{i,\alpha}[(X - G_i)^\alpha - \overline{(X - G_i)^\alpha}]$$

and where $\overline{\mathcal{P}_{i,j}}$ stands for the mean of $\mathcal{P}_i(X)$ on cell j.

For the Euler model (6), the CENO scheme writes:

$$\text{Find } u_0 \in \mathcal{V}_0 \text{ such that } B(R_2^0 u_0, v_0) \;=\; 0 \;\forall\; v_0 \in \mathcal{V}_0 \tag{7}$$

We observe that this produces a finite volume formulation:

$$\forall C_i, \quad \int_{C_i} \nabla \cdot \mathcal{F}(R_2^0 u_0)\; d\;\Omega \;-\; \int_{\partial C_i \cap \Gamma} \mathcal{F}_\Gamma(R_2^0 u_0)\; d\;\Gamma \;=\; 0.$$

or:

$$\forall C_i, \quad \int_{\partial C_i} \mathcal{F}(R_2^0 u_0) \cdot \mathbf{n}\; d\;\Gamma - \int_{\partial C_i \cap \Gamma} \mathcal{F}_\Gamma(R_2^0 u_0)\; d\;\Gamma \;=\; 0. \tag{8}$$

The knowledge of the reconstruction does not completely define the CENO approximation. Indeed, the reconstruction performed in each cell produces a global field which is generally discontinuous at cell interfaces. In order to fix an integration value at the interface, we can consider an arithmetic mean of the fluxes values for the two reconstruction values:

$$\mathcal{F}(R_2^0 u_0)^{quadrature}|_{\partial C_i \cap \partial C_j} \cdot \mathbf{n} = \frac{1}{2}\left(\mathcal{F}(R_2^0 u_0)|_{\partial C_i} + \mathcal{F}(R_2^0 u_0)|_{\partial C_j}\right) \cdot \mathbf{n} \tag{9}$$

where $(R_2^0 u_0)|_{\partial C_i}$ holds for the value at cell boundary of the reconstructed $R_2^0 u_0|_{C_i}$ on cell C_i. The above mean is applied on Gauss integration points (two per interface segment). This formulation produces a central-differenced numerical approximation which is third order accurate, but it cannot be used as it is in nonlinear applications, due to a lack of stability.

3.3. Vertex-centered low dissipation CENO2

Scheme (8) is usually combined with an approximate Riemann solver used instead of (9). This latter option produces a rather dissipative third-order accurate scheme. Now, we are here interested only by rather mild non-linear effects. Scheme (8)(9) is instead stabilized as in [1], *i.e* completed by two extra terms: the first term compensates partially the main dispersive error. The second one introduces a sixth order dissipation. We refer to [1] for details and for numerical experiments showing the interest of this new CENO2 variant. This modification does not change the main error term in the approximation and will not influence our error analysis.

4. Error analysis

Let be $j(u) = (g, u)$ the scalar output which we want to accurately compute, where u is the solution of the continuous system (6). We concentrate the reduction by mesh adaption of the following

error:

$$\delta j = (g, R_2^0\pi_0 u - R_2^0 u_0)$$

where g is function of $L^2(\Omega)$ and u_0 the discrete solution of (8). The projection π_0: is defined by:

$$\begin{aligned} \pi_0 : (V) &\to (V_0), \\ v &\mapsto \pi_0 v \\ \forall\ C_i, \text{dual cell}, \pi_0 v|_{C_i} &= \int_{C_i} v dx. \end{aligned}$$

The adjoint state $u_0^* \in \mathcal{V}_0$ is the solution of:

$$\frac{\partial B}{\partial u}(R_2^0 u_0)(R_2^0 v_0, u_0^*) = (g, R_2^0 v_0),\ \forall\ v_0 \in \mathcal{V}_0. \tag{10}$$

Then we can write, successively:

$$\begin{aligned} (g, R_2^0\pi_0 u - R_2^0 u_0) &= \tfrac{\partial B}{\partial u}(R_2^0 u_0)(R_2^0\pi_0 u - R_2^0 u_0, u_0^*) \quad \text{(adjoint eq.)(10)} \\ &\approx B(R_2^0\pi_0 u, u_0^*) - B(R_2^0 u_0, u_0^*) \end{aligned}$$

and then

$$\begin{aligned} &(g, R_2^0\pi_0 u - R_2^0 u_0) \\ &\qquad \approx \quad B(R_2^0\pi_0 u, u_0^*) \qquad \text{(disc.state eq.)(7)(9)} \\ &\qquad \approx \quad B(R_2^0\pi_0 u, u_0^*) - B(u, u_0^*) \quad \text{(cont.state eq.)(6)} \\ &\qquad \approx \quad \tfrac{\partial B}{\partial u}(u)(R_2^0\pi_0 u - u, u_0^*) \end{aligned}$$

In this study, *we do not consider the adaptation of boundary mesh* therefore, as in [20], we discard the boundary terms. Then the case of Euler equations is written:

$$\begin{aligned} \frac{\partial B}{\partial u}(u)(R_2^0\pi_0 u - u, u_0^*) &= \sum_i \int_{C_i} u_0^* \nabla \cdot \mathcal{F}'(u)(R_2^0\pi_0 u - u) dx - \int_{\partial C_i \cap \Gamma} u_0^* \mathcal{F}'_\Gamma(u)(R_2^0\pi_0 u - u)\ d\ \Gamma \\ &\approx \sum_i \int_{C_i} u_0^* \nabla \cdot \mathcal{F}'(u)(R_2^0\pi_0 u - u) dx \end{aligned}$$

where the sum applies for all dual cell C_i of the mesh. Noting that u_0 is constant over each cell C_i, we can transform the above with an integration by parts (again terms on $\partial\Omega$ are skipped):

$$\frac{\partial B}{\partial u}(u)(R_2^0\pi_0 u - u, u_0^*) \approx -\sum_i \int_{\partial C_i} u_0^* \mathcal{F}'(R_2^0\pi_0 u - u) \cdot \mathbf{n}\ \mathrm{d}\sigma.$$

Observing that two integrals are computed on each interface C_{ij} separating two neighboring cells:

$$\frac{\partial B}{\partial u}(u)(R_2^0\pi_0 u - u, u_0^*) \approx -\sum_{C_{ij}} \int_{\partial C_i \cap \partial C_j} \left[\left(u_0^* \mathcal{F}'(R_2^0\pi_0 u - u)\right)_{C_i} - \left(u_0^* \mathcal{F}'(R_2^0\pi_0 u - u)\right)_{C_j} \right] \cdot \mathbf{n}\ \mathrm{d}\sigma.$$

Even for $u_0^* \approx \pi_0 u^*$, with u^* smooth, the discontinuity at interface of u_0^* is of order 1. By construction of the higher order reconstruction, the discontinuity at interface of $R_2^0\pi_0 u - u$ is of higher order and can be neglected. Then:

$$\left(u_0^* \mathcal{F}'(R_2^0\pi_0 u - u)\right)_{C_i} - \left(u_0^* \mathcal{F}'(R_2^0\pi_0 u - u)\right)_{C_j} \approx \\ \frac{1}{2}\left[(u_0^*)_{C_i} - (u_0^*)_{C_j}\right]\left[\left(\mathcal{F}'(R_2^0\pi_0 u - u)\right)_{C_i} + \left(\mathcal{F}'(R_2^0\pi_0 u - u)\right)_{C_j}\right]$$

We assume in this work that $R_2^0\pi_0 u - u$ can be replaced by a smooth function of the local third derivatives and local mesh size:

$$R_2^0\pi_0 u_q - u_q \approx \sup_{\delta\mathbf{x}} \sup_{\mathbf{x}} |D^3 u(\mathbf{x})(\delta\mathbf{x})^3|, \quad \forall\ q = 1, 4,$$

and for each flux component ($r = 1, 2$)

$$\mathcal{F}'_r(R_2^0\pi_0 u - u) \approx \sum_q\ ||\mathcal{F}'_{qr}||(D^3 u(\mathbf{x})(\delta\mathbf{x})^3).$$

On the other side, the jump term $u_0^*|_{C_i} - u_0^*|_{C_j}$ is a first derivative of u^* times the distance between the centroids of the two cells, or equivalently (at first-order) the vertices i and j. The integration of this term over the section of interface $\partial C_i \cap \partial C_j$ is essentially the (double of the) area of the four triangles delimited by i, j and the centroids of triangles havin ij as common side. The set of all these triangles is a tessellation of the computational domain. Then:

$$|\delta j| \approx |\frac{\partial B}{\partial u}(u)(R_2^0\pi_0 u - u, u_0^*)| \approx 2\sum_q \int_\Omega K_q(u, u^*)|D^3 u(\delta\mathbf{x})^3)|\ \mathrm{d}\Omega$$

with

$$K_q(u, u^*) = \sum_r |(\mathcal{F}'_{rq}(u))^*||\frac{\partial u_q^*}{\partial x_r}|.$$

The error is expressed in terms of the $\delta\mathbf{x}$, measuring local mesh size. We consider now a way to find the mesh which minimizes this error.

Metric parametrization

The parametrization of the mesh is a Riemannian metric defined in each point $\mathbf{x} = (x, y)$ of the computational domain by a symmetric matrix,

$$\mathcal{M}(\mathbf{x}) = d\ \mathcal{R}(\mathbf{x})\Lambda(\mathbf{x})\mathcal{R}^t(\mathbf{x}).$$

The rotation matrix $\mathcal{R} = (\mathbf{e}_\xi, \mathbf{e}_\eta)$, built with the normalised eigenvectors $\mathbf{e}_\xi = (e_\xi^x, e_\xi^y)$ and $\mathbf{e}_\eta = (e_\eta^x, e_\eta^y)$ of $\mathcal{M}$, parametrizes the two orthogonal stretching directions of the metric. Denoting m_ξ and m_η the two directional local mesh sizes in the characteristic/stretching directions of $\mathcal{M}$, the mesh density is $d = (m_\xi m_\eta)^{-1}$. Matrix Λ is a 2×2 diagonal one with eigenvalues $\lambda_1 = \frac{m_\xi}{m_\eta}$ and $\lambda_2 = \frac{m_\eta}{m_\xi}$ and of determinant equal to unity, which helps defining uniquely the mesh density d from matrix $\mathcal{M}$. It is also useful to identify the mesh sizes $(\delta x, \delta y)$ in Cartesian directions:

$$\delta \mathbf{x}_\mathcal{M} = (\delta x_\mathcal{M}, \delta y_\mathcal{M}) \quad , \quad \delta x_\mathcal{M} = e_\xi^x m_\xi + e_\eta^x m_\eta \quad , \quad \delta y_\mathcal{M} = e_\xi^y m_\xi + e_\eta^y m_\eta \ .$$

In the continuous mesh methods (see for example [17, 18], the error in linear interpolation was modelled by (we discard the constant):

$$\begin{aligned} |u_q(\mathbf{x}) - \pi_1^\mathcal{M} u_q(\mathbf{x})| \ &\approx \ |\frac{\partial^2 u_q}{\partial \tau_q^2}|(\delta\tau_q)^2 + |\frac{\partial^2 u_q}{\partial n_q^2}|(\delta n_q)^2 \ = \ \delta \mathbf{x}_\mathcal{M} |H_{u_q}| \delta \mathbf{x}_\mathcal{M} \\ &= \ trace(\mathcal{M}^{-\frac{1}{2}} |H_{u_q}| \mathcal{M}^{-\frac{1}{2}}) \end{aligned} \tag{11}$$

where H_{u_q} is the Hessian of u_q, and orthonormal directions $\tau_q = (\tau_x^q, \tau_y^q)$ and $n_q = (n_x^q, n_y^q)$ are eigenvectors of this Hessian.

In [21] the authors propose a general statement for an interpolation of arbitrary degree generalizing (11). Here, we directly define the error model for a quadratic reconstruction as follows (for $q = 1, 4$):

$$|u_q(\mathbf{x}) - \pi_2 u_q(\mathbf{x})| \approx \left(trace(\mathcal{M}^{-\frac{1}{2}} |\tilde{H}_{u_q}| \mathcal{M}^{-\frac{1}{2}}) \right)^{\frac{3}{2}} \ .$$

where the pseudo-Hessian $\tilde{H}_{u_q}$ has to be derived numerically from the third derivative as explained in the numerical application section. After the *a priori* analysis, we have to minimise the following error:

$$\begin{aligned} \mathcal{E} \ &= \ \sum_{q=1,4} \int K_q(u, u^*) \left(trace(\mathcal{M}^{-\frac{1}{2}} |\tilde{H}_{u_q}| \mathcal{M}^{-\frac{1}{2}}) \right)^{\frac{3}{2}} \ dxdy \ . \\ &\preceq \ \int \left(trace(\mathcal{M}^{-\frac{1}{2}} |S| \mathcal{M}^{-\frac{1}{2}}) \right)^{\frac{3}{2}} \ dxdy. \end{aligned}$$

with

$$S = \sum_{q=1,4} K_q(u, u^*)^{\frac{2}{3}} |\tilde{H}_{u_q}|. \tag{12}$$

Matrix $S(\mathbf{x})$ is a sum of symmetric positive definite matrices and so is it:

$$S(\mathbf{x}) = \mathcal{R}_S(\mathbf{x}) \Lambda_S(\mathbf{x}) \mathcal{R}_S^t(\mathbf{x}).$$

Optimal metric. We know identify the optimal metric, $\mathcal{M}^{opt} = \mathcal{M}^{opt}(N)$, among those having a prescribed total node number N, which minimizes the above error. We proceed as for the second-order metric analysis, e.g. [20].

We observe that:

$$\int \left(trace(\mathcal{M}^{-\frac{1}{2}}|S|\mathcal{M}^{-\frac{1}{2}})\right)^{\frac{3}{2}} \; dxdy = \int \left(trace(d_{\mathcal{M}}^{-1}(\mathcal{R}_{\mathcal{M}}\Lambda_{\mathcal{M}}\mathcal{R}_{\mathcal{M}}^{T})^{-\frac{1}{2}}|S|(\mathcal{R}_{\mathcal{M}}\Lambda_{\mathcal{M}}\mathcal{R}_{\mathcal{M}}^{T})^{-\frac{1}{2}})\right)^{\frac{3}{2}} \; dxdy$$

Mesh stretching direction. We first prescribe, at each point $\mathbf{x}$ of the computational domain, the adapted metric eigenvectors *i.e.* the representation of the direction of stretching of mesh, $\mathcal{R}_{\mathcal{M}_{opt}}$ as aligned with the above error model, that is

$$\mathcal{R}_{\mathcal{M}_{opt}} = \mathcal{R}_{\mathcal{S}}.$$

Mesh stretching strength. Then, minimising the error at each point $\mathbf{x}$ of the computational domain for a prescribed density $d_{\mathcal{M}}$, we derive that the best ratio of eigenvalues for $\mathcal{M}$, *i.e.* the representation of mesh stretching or anisotropy should uniformise the two component of error, which means that the product

$$(\mathcal{R}_{\mathcal{M}_{opt}}\Lambda_{\mathcal{M}_{opt}}\mathcal{R}_{\mathcal{M}_{opt}}^{T})^{-\frac{1}{2}}|S|(\mathcal{R}_{\mathcal{M}_{opt}}\Lambda_{\mathcal{M}_{opt}}\mathcal{R}_{\mathcal{M}_{opt}}^{T})^{-\frac{1}{2}}$$

is made proportional to identity. It implies that:

$$e_{\mathcal{M}_{opt}} = \frac{(\lambda_{1_S})^{-\frac{1}{2}}}{(\lambda_{2_S})^{-\frac{1}{2}}} \; ; \; \Lambda_{\mathcal{M}_{opt}} = diag[e_{\mathcal{M}_{opt}}^{-1}, e_{\mathcal{M}_{opt}}]$$

in which we have respected $det(\Lambda_{\mathcal{M}_{opt}}) = 1$.

With these definitions of $\mathcal{R}_{\mathcal{M}_{opt}}$ and $\Lambda_{\mathcal{M}_{opt}}$, we get:

$$(\mathcal{R}_{\mathcal{M}_{opt}}\Lambda_{\mathcal{M}_{opt}}\mathcal{R}_{\mathcal{M}_{opt}}^{T})^{-\frac{1}{2}}|S|(\mathcal{R}_{\mathcal{M}_{opt}}\Lambda_{\mathcal{M}_{opt}}\mathcal{R}_{\mathcal{M}_{opt}}^{T})^{-\frac{1}{2}} \; = \; \begin{pmatrix} \lambda_{1_S}^{\frac{1}{2}}\lambda_{2_S}^{\frac{1}{2}} & 0 \\ 0 & \lambda_{1_S}^{\frac{1}{2}}\lambda_{2_S}^{\frac{1}{2}} \end{pmatrix}.$$

Inside this restricted family of metrics, it remains to define the optimal metric density. Let us consider the set of metrics with a total number of vertices prescribed to N:

$$\int_{\Omega} d \; dxdy = N. \tag{13}$$

We now have to minimise the L^1 norm of the error

$$\begin{aligned} \mathcal{E}(d) &= \int_{\Omega} d^{-\frac{3}{2}}\Gamma(S) \; dxdy \\ \Gamma(S) &= \left(trace\begin{pmatrix} \lambda_{1_S}^{\frac{1}{2}}\lambda_{2_S}^{\frac{1}{2}} & 0 \\ 0 & \lambda_{1_S}^{\frac{1}{2}}\lambda_{2_S}^{\frac{1}{2}} \end{pmatrix}\right)^{\frac{3}{2}} = (2\lambda_{1_S}^{\frac{1}{2}}\lambda_{2_S}^{\frac{1}{2}})^{\frac{3}{2}} \end{aligned} \tag{14}$$

with respect to d for a given number of nodes N. This means that:

$$\mathcal{E}'(d)\cdot\delta d = 0 \;\;\forall\;\; \delta d \;\; \text{with} \int_\Omega \delta d \; dxdy = 0$$

which implies that the derivative of integrand in $\mathcal{E}$ is constant:

$$\Gamma(S) d^{-\frac{5}{2}} = constant$$

and produces an optimal density

$$d_{opt} = \frac{N}{C}_{opt} (\Gamma(S))^{\frac{2}{5}} = \frac{N}{C}_{opt} (2\lambda_{1_S}^{\frac{1}{2}} \lambda_{2_S}^{\frac{1}{2}})^{\frac{3}{5}}$$

with

$$C_{opt} = \int_\Omega (2\lambda_{1_S}^{\frac{1}{2}} \lambda_{2_S}^{\frac{1}{2}})^{\frac{3}{5}} \; dxdy.$$

This completes the definition of the optimal metric:

$$\mathcal{M}_{opt} = d_{opt} \mathcal{R}_{opt}^t \begin{pmatrix} e_{opt}^{-1} & 0 \\ 0 & e_{opt} \end{pmatrix} \mathcal{R}_{opt}. \tag{15}$$

Numerical experiments are presented in [10].

5. Norm-oriented analysis

5.1. Corrector

We consider an abstract linear PDE denoted $Au = f$ and a third-order accurate discretization of it, $A_h u_h = f_h$. Let us assume the problem is smooth and that the approximation is in its asymptotic mesh convergence phase for the mesh Ω_h under study, of size h. Then this will be also true for a strictly two-times finer embedding mesh $\Omega_{h/2}$. We would have:

$$\begin{aligned} u_h = A_h^{-1} f_h \quad , \quad u_{h/2} = A_{h/2}^{-1} f_{h/2} \\ \Rightarrow \quad u - u_{h/2} \approx \frac{1}{8}(u - u_h) \end{aligned} \tag{16}$$

where u_h and $u_{h/2}$ are respectively the solutions on Ω_h and $\Omega_{h/2}$. We have also $\Pi_h u - \Pi_h u_{h/2} \approx \frac{1}{8}(\Pi_h u - u_h)$. This motivates the definition of a finer-grid Defect-Correction (DC) corrector as follows:

$$A_h \bar{u}'_{DC} = \frac{8}{7} R_{h/2\to h}(A_{h/2} P_{h\to h/2} u_h - f_{h/2}) \tag{17}$$

where the residual transfer $R_{h/2\to h}$ accumulates on coarse grid vertices the values at fine vertices in neighboring coarse elements multiplied with barycentric weights, and $P_{h\to h/2}$ linearly interpolates

coarse values on fine mesh. In the case of local singularities, statement (16) is not true for uniform meshes, but we have some hints that it holds almost everywhere for a sequence of adapted meshes, according to [20]. The DC corrector $\bar{u}'_{DC}$ approximates $\Pi_h u - u_h$ instead of $u - u_h$ and can be corrected as the previous one:

$$u'_{DC} = \bar{u}'_{DC} - (\pi_h u_h - u_h). \tag{18}$$

This field will play a key role in the norm-oriented mesh adaptation introduced in the sequel.

This method can be extended to Euler flow adaptation. Let us denote $\Psi(W) = 0$ the steady Euler equations where $W = \{\rho, \rho\mathbf{u}, \rho E\}$ is the set of conservation variables. Let $\Psi_h(W_h) = 0$ be its discretization by a vertex-centered second-order upwind scheme. A linear DC evaluation of the corrector writes:

$$\begin{aligned} \frac{\partial \Psi_h}{\partial W}\bar{W}'_{DC} &= \frac{8}{7} R_{h/2\to h}\Psi_{h/2}(P_{h\to h/2}W_h), \\ W'_{DC} &= \bar{W}'_{DC} - (\pi_h W_h - W_h). \end{aligned} \tag{19}$$

Then

$$\frac{\partial \Psi_h}{\partial W} g'_{DC} = W'_{DC}. \tag{20}$$

In practice, a *nonlinear* version of (20) is used.

5.2. Norm-oriented optimal metric

We are now interested by the minimization of $\delta j(\mathcal{M}) = ||u - u_{\mathcal{M}}||^2_{L^2(\Omega)}$ with respect to the mesh $\mathcal{M}$. Introducing u'_{DC} from (18) gives:

$$\delta j(\mathcal{M}) \approx (u'_{DC}, u - u_{\mathcal{M}}). \tag{21}$$

Let us define the discrete adjoint state $u^*_{\mathcal{M}}$:

$$\forall \psi \in V_{\mathcal{M}}, \quad B(\psi_{\mathcal{M}}, u^*_{\mathcal{M}}) = (\psi_{\mathcal{M}}, u'_{DC}). \tag{22}$$

Then, similarly to the goal-oriented case, we have to solve the following optimum problem.

$$\begin{aligned} \mathcal{E} &= \sum_{q=1,4} \int K_q(u, u^*_{\mathcal{M}}) \left(trace(\mathcal{M}^{-\frac{1}{2}} |\tilde{H}_{u_q}| \mathcal{M}^{-\frac{1}{2}}) \right)^{\frac{3}{2}} \; dxdy \; . \\ &\preceq \int \left(trace(\mathcal{M}^{-\frac{1}{2}} | \sum_{q=1,4} K_q(u, u^*_{\mathcal{M}})^{\frac{2}{3}} |\tilde{H}_{u_q}| | \mathcal{M}^{-\frac{1}{2}}) \right)^{\frac{3}{2}} dxdy. \end{aligned}$$

Exactly as in other norm-oriented analyses, we freeze the dependancy of the adjoint state to metric $\mathcal{M}$ by replacing it by $\mathcal{M}_0$, fixed.

$$\min_{\mathcal{M}} \int \left(trace(\mathcal{M}^{-\frac{1}{2}} | \sum_{q=1,4} K_q(u, u^*_{\mathcal{M}_0})^{\frac{2}{3}} |\tilde{H}_{u_q}| | \mathcal{M}^{-\frac{1}{2}}) \right)^{\frac{3}{2}} dxdy.$$

In order to get the final norm-oriented optimum $\mathcal{M}_{opt,norm}$ we shall:

Step 1: first solve the linearised corrector system (18) in order to get u'_{DC},

Step 2: then solve the adjoint system:

$$B(\psi, u^*_{\mathcal{M}}) = (\psi, u'_{DC}) \tag{23}$$

Step 3: Define $\mathcal{M}^{(\alpha+1)}$ as in (15). the three-step process being re-iterated until we get a fixed point $\mathcal{M}_{opt,norm} = \mathcal{M}^{(\infty)}$.

6. Conclusion

The proposed analysis is being implemented. Details of implementation and numerical results will be published in a forthcoming paper.

7. Acknowledgements

This work has been supported by French National Research Agency (ANR) through COSINUS program (project ECINADS n^o ANR-09-COSI-003) and MAIDESC n^o ANR-13-MONU-0010.

References

[1] A. Dervieux A. Carabias, O. Allain. Dissipation and dispersion control of a quadratic-reconstruction advection scheme. In *In European Workshop on High Order Nonlinear Numerical Methods for Evolutionary PDEs: Theory and Applications*, Trento, Italy, april 11-15 2011.

[2] T. Apel. *Anisotropic finite elements: Local estimates and applications.* Book Series: Advances in Numerical Mathematics. Teubner, Stuttgart, 1999.

[3] T.J. Barth. Recent developements of high-order k-exact reconstruction on unstructured meshes. In *31st AIAA Aerospace Science Meeting*, AIAA-93-0668, Reno, NV, USA, 1993.

[4] T.J. Barth and M.G. Larson. A-posteriori error estimation for higher order godunov finite volume methods on unstructured meshes. In R. Herbin and D. Kröner, editors, *Finite Volumes for Complex Applications III*, pages 41–63. 41 63, 2002.

[5] A. Belme, F. Alauzet, and A. Dervieux. A priori anisotropic goal-oriented estimate and mesh adaptation for viscous compressible flow. *Preprint*, 2012.

[6] A. Belme, A. Dervieux, and F. Alauzet. A fully anisotropic goal-oriented mesh adaptation for unsteady flows. In *Proceedings of the V ECCOMAS CFD Conf.*, 2010.

[7] G. Brethes, O. Allain, and A. Dervieux. A mesh-adaptative metric-based full-multigrid for the poisson problem. *Int. J. Numer. Meth. Fluids*, 2015.

[8] G. Brethes, A. Loseille, F. Alauzet, and A. Dervieux. Estimates- and corrector-based mesh adaptation. In *PANACM 2015*, 2015.

[9] Weiming Cao. An interpolation error estimate on anisotropic meshes in r^n and optimal metrics for mesh refinement. *SIAM J. Numer. Anal.*, 45(6):2368 2391, 2007.

[10] A. Carabias. *Analyse et adaptation de maillage pour des schémas non-oscillatoires d'ordre élevé.* PhD thesis, Université de Nice-Sophia-Antipolis, 2013. (in French).

[11] P.G. Ciarlet and P.A. Raviart. General Lagrange and Hermite interpolation in Frn with applications to finite element methods. *Archive for Rational Mechanics and Analysis*, 46:177–199.

[12] L. Formaggia, S. Micheletti, and S. Perotto. Anisotropic mesh adaptation in computational fluid dynamics: Application to the advection-diffusion-reaction and the Stokes problems. *Appl. Numer. Math.*, 51(4):511–533, 2004.

[13] I. Abalakin B. Koobus H. Ouvrard, T. Kozubskaya and A. Dervieux. Advective vertex-centered recon- struction scheme on unstructured meshes. RR-7033, INRIA, 2009.

[14] L. Ivan and C. P. T. Groth. High-order central eno finite-volume scheme with adaptive mesh refinement. In *18th AIAA Computational Fluid Dynamics Conference*, AIAA-2007-4323, 25 - 28 June 2007, Miami, FL, 2007.

[15] G. Kunert. *A Posteriori Error Estimation for Anisotropic Tetrahadral and Triangular Finite Element Meshes*. PhD thesis, Fakultatur Mathematik der Technischen Universita, Chemnitz, Germany, 1999.

[16] A. Loseille. *Adaptation de maillage anisotrope 3D multi-échelles et ciblée à une fonctionnelle pour la mécanique des fluides. Application à la prédiction haute-fidélité du bang sonique*. PhD thesis, Université Pierre et Marie Curie, Paris VI, Paris, France, 2008. (in French).

[17] A. Loseille and F. Alauzet. Continuous mesh framework. Part I: well-posed continuous interpolation error. *SIAM Num. Anal.*, 49(1):38–60, 2011.

[18] A. Loseille and F. Alauzet. Continuous mesh framework. Part II: validations and applications. *SIAM Num. Anal.*, 49(1):61–86, 2011.

[19] A. Loseille, A Dervieux, and F. Alauzet. Anisotropic norm-oriented mesh adaptation for compressible flows. In *53rd AIAA Aerospace Sciences Meeting*, 2015.

[20] A. Loseille, A. Dervieux, P.J. Frey, and F. Alauzet. Achievement of global second-order mesh convergence for discontinuous flows with adapted unstructured meshes. In *37th AIAA Fluid Dynamics Conference and Exhibit*, AIAA-2007-4186, Miami, FL, USA, Jun 2007.

[21] E. Mbinky, F. Alauzet, and A. Loseille. High order interpolation ofr mes adaptation. In *Proceedings of ECCOMAS CFD*, Vienna, Austria, 2012.